This article has been accepted for publication in a future issue of this journal, but has not been fully edited. Content may change prior to final publication. Citation information: DOI 10.1109/ACCESS.2018.2872953, IEEE Access



# Partially-Activated Conjugate Beamforming for LoS Massive MIMO Communications

Wendong Liu, *Student Member, IEEE*, Zhaocheng Wang, *Senior Member, IEEE*, Jianfei Cao, Sheng Chen, *Fellow, IEEE*, and Lajos Hanzo, *Fellow, IEEE*

***Abstract*—A partially-activated conjugate beamforming (PACB) is proposed for massive multiple-input multiple-output (MIMO) communications where the line-of-sight (LoS) channel is dominant. Unlike the conventional conjugate beamforming which activates all the antenna elements to radiate the signals, our PACB activates only a fraction of the antennas by exploiting the spatial structure of LoS channel, and it can mitigate the inter-user interference more effectively, leading to dramatically enhanced downlink spectral efficiency. A low-complexity search algorithm is also introduced to calculate the optimal number of activated antennas. Theoretical analysis and simulation results both confirm that our PACB offers significantly higher downlink spectral efficiency compared to its conventional beamforming counterpart.**

***Index Terms*—Partially-activated conjugate beamforming, line-of-sight, massive MIMO, inter-user interference**

## I. Introduction

Massive multiple-input multiple-output (MIMO) offers a promising technology for the next generation wireless communication systems [1]–[4]. Because the asymptotic orthogonality is achievable by employing a large-scale antenna array at the base station (BS), massive MIMO is capable of enhancing both the spectral and energy efficiencies significantly with the aid of linear signal processing [2]. For example, the conjugate beamforming (CB) can be utilized to effectively eliminate the inter-user interference (IUI) between the uncorrelated channels from different users [3]. To ensure the asymptotic orthogonality requires the rich-scattering channel environment, which is generally the case in current wireless communication systems. In this case, the non-line-of-sight (NLoS) component is dominant and the wireless channel can be modeled approximately by a Gaussian distribution with low correlation between different users [1], [2]. To fully explore the potential of spatial diversity and multiplexing gains provided by NLoS channels, advanced beamforming and precoding methodologies have been proposed to enhance the performance of massive MIMO systems [3], [5]–[7].

However, in many new wireless communication applications, the line-of-sight (LoS) channel is dominant. For example, in air-to-air communications, the LoS channel is predominant with litter or no scattering component [8]. Also LoS channels are widely approved in unmanned aerial vehicle (UAV) communications [9], [10]. Firstly, LoS links in low-altitude UAV-ground channels are mostly preferred [10]. In addition, the UAV-UAV and UAV-BS backhaul channels are dominated by LoS components as well, wherein the emerging millimeter-wave (mmWave) MIMO technology is utilized to achieve the high-rate transmissions [9]. In mmWave communications, the pathloss of NLoS channels is relatively high, and LoS signals are mainly considered [11]–[13]. The asymptotic orthogonality is invalid in LoS scenarios due to the higher correlation between various channels from different users [12], which results in higher residual IUI and spectral efficiency (SE) loss. Thus the conventional low-complexity analogue CB suffers from serious performance degradation in LoS environments, and the hybrid precoding architecture is often preferred [14], [15]. But the joint design of digital and analogue precoders/combiners is a complicated optimization with inherently high complexity [14]–[16]. Moreover, since 5G new radio (NR) requires larger user density and higher SE, serving adjacent users at the same time-frequency resource draws lots of attentions recently [17], [18]. As claimed in [17], non-linear precoding including Tomlinson-Harashima precoding (THP) and vector perturbation (VP) should be investigated to enhance the MU-MIMO performance with adjacent users. However, non-linear precoding methodologies possess high complexity and major channel state information (CSI)-related modifications in practical massive MIMO systems [19]. This motivates us to investigate the efficient low-complexity alternative to the conventional CB, capable of applying to LoS massive MIMO communications, especially with adjacent users.

In this paper, we reveal a fascinating property of LoS scenario, namely, adopting transmit antennas as many as possible for CB may not be a good choice, and using a smaller number of transmit antennas is often capable of mitigating the IUI more effectively. Based on this discovery, a partially-activated conjugate beamforming (PACB) scheme is proposed to exploit the spatial structure of the LoS channel by activating only a fraction of all the antennas, which we prove is capable of realizing a better orthogonality of the channels for different users.

W. Liu and Z. Wang are with Tsinghua National Laboratory for Information Science and Technology, Department of Electronic Engineering, Tsinghua University, Beijing 100084, P.R. China (Emails: lwd15@mails.tsinghua.edu.com, zcwang@mail.tsinghua.edu.cn)

J. Cao is with SONY China Research Laboratory, Beijing 100190, China (Email: jeffrey.cao@sony.com.cn)

S. Chen and L. Hanzo are with School of Electronics and Computer Science, University of Southampton, Southampton SO17 1BJ, U.K. (Emails: sqc@ecs.soton.ac.uk, lh@ecs.soton.ac.uk). S. Chen is also with King Abdulaziz University, Jeddah 21589, Saudi Arabia.

This work was supported in part by National Natural Science Foundation of China (Grant No. 61571267), in part by National High Technology Research and Development Program of China (Grant No. 2014AA01A704), in part by Shenzhen Peacock Plan (No. 1108170036003286), and in part by Shenzhen Visible Light Communication System Key Laboratory (ZDSYS20140512114229398).

L. Hanzo gratefully acknowledges the financial support of the EPSRC projects EP/Noo4558/1, EP/PO34284/1, of the Royal Society's GRCF as well as of the European Research Council's Advanced Fellow Grant QuantCom.

Specifically, we prove that by activating a fraction of all the antennas for beamforming, the amplitude of the inner-product between the channel vectors of two different users is much closer to zero, compared to the case of adopting all the antennas for beamforming. Thus, the IUI is reduced considerably and the signal-to-interference plus noise ratio (SINR) is improved significantly. The optimal number of activated antennas can be determined by maximizing the system's capacity or SINR using an exhaustive search, which has the complexity on the order of $\mathsf{O}(M_{\rm t})$, where $M_{\rm t}$ is the number of available antennas. A even lower complexity search algorithm is also derived to calculate the number of the activated antennas by maximizing the system's signal-to-interference ratio (SIR). Both theoretical analysis and simulation study confirm that the system's SE achieved by this low-complexity search is indistinguishable from the optimal performance attained by the exhaustive search under high signal-to-noise ratio (SNR) conditions. Theoretical analysis and simulation results also validate the superior SE of our PACB scheme over the conventional CB.

It must be pointed out that our PACB for LoS massive MIMO is completely different from the subset antenna selection for MIMO under a rich-scattering environment. In the latter case, to reduce the required radio-frequency (RF) chains to $N$, where $N < M_{\rm t}$, subset antenna selection is carried out to select a subset of $N$ antennas from the full set of $M_{\rm t}$ antennas [20]. The optimal subset antenna selection has the complexity on the order of $\mathsf{O}\left(\binom{M_{\rm t}}{N}\right)$, which is impossible to do even for a modest $M_{\rm t}$. Critically, in rich-scattering environments, the performance of the optimal $N$-antenna system is always worst than that of the full $M_{\rm t}$-antenna system. By contrast, in LoS environments, our PACB with a complexity much lower than $\mathsf{O}(M_{\rm t})$ simply activates the first $N_{\rm o}$ antennas, and its performance is better than that of employing all the $M_{\rm t}$ antennas. The recent works [21], [22] randomly select $N$ antennas from the full set of $M_{\rm t}$ antennas to enhance mmWave communication security, which is obviously different from our PACB.

## II. System Model

### A. Transmission and Channel Model

Consider a mmWave BS employs a uniformly-spaced linear array (ULA) having $M_{\rm t}$ transmit antennas to support $I$ mobile users using the same time/frequency resource block. To highlight the underlying physics and without loss of generality, we restrict our analysis mainly to the case of $I = 2$. However, latter we will extend our PACB to the generic case of $I > 2$.

Each user is equipped with a ULA of $M_{\rm r}$ antennas. Denote $\boldsymbol{H}_i \in \mathbb{C}^{M_{\rm r}\times M_{\rm t}}$ as the downlink channel matrix between the BS and the $i$th user, and let $x_i$ be the transmitted symbol to user $i$, where $i = 1, 2$. The BS performs the transmit beamforming on $x_i$ with the beamforming vector $\boldsymbol{f}_i \in \mathbb{C}^{M_{\rm t}\times 1}$. The total power constraint with $E\{\boldsymbol{x}\boldsymbol{x}^{\rm H}\} = \frac{1}{2}\boldsymbol{I}_2$ and $||\boldsymbol{F}||_{\rm F}^2 = 2$ are utilized [14], wherein $E\{\cdot\}$ and $||\cdot||_{\rm F}$ represent the expectation and Frobenius norm, respectively. $\boldsymbol{x} = [x_1, x_2]^{\rm T}$ is the transmitted symbol vector and $\boldsymbol{F} = [\boldsymbol{f}_1, \boldsymbol{f}_2]$ denotes the beamforming matrix at the BS. User $i$ carries out the combining operation on the signals received at its $M_{\rm r}$ antennas with the combining vector $\boldsymbol{w}_i \in \mathbb{C}^{M_{\rm r}\times 1}$. Thus, the received symbol $y_i$ by the $i$th user can be expressed as

$$y_i = \boldsymbol{w}_i^{\rm T}\boldsymbol{H}_i\boldsymbol{f}_i x_i + \boldsymbol{w}_i^{\rm T}\boldsymbol{H}_i\boldsymbol{f}_{i'}x_{i'} + n_i,\ i, i' = 1, 2,\ i' \neq i, \quad (1)$$

where $(\cdot)^{\rm T}$ denotes the transpose operator, and $n_i$ is the additive white Gaussian noise (AWGN) with power $\sigma_n^2$. The term $\boldsymbol{w}_i\boldsymbol{H}_i\boldsymbol{f}_{i'}x_{i'}$ represents the IUI.

The channel model for $\boldsymbol{H}_i$ is given by [14]

$$\boldsymbol{H}_i = \gamma\sum_{p=0}^{P}\alpha_p\boldsymbol{H}_{i,p} = \gamma\sum_{p=0}^{P}\alpha_p\boldsymbol{h}_{\rm r}(\theta_{i,p})\boldsymbol{h}_{\rm t}^{\rm T}(\varphi_{i,p}), \quad (2)$$

in which $\boldsymbol{H}_{i,0}$ and $\boldsymbol{H}_{i,p}, 1 \leq p \leq P$ represent the LoS and NLoS channel components, respectively, wherein $P$ is the total number of NLoS sub-paths. $\alpha_p$ denotes the complex gain associated with the $p$-th sub-path. $\gamma$ is the channel normalization factor to ensure $E\{||\boldsymbol{H}_i||_{\rm F}^2\} = M_{\rm t}M_{\rm r}$. Furthermore, with antenna spacing $D = \lambda/2$, where $\lambda$ is the carrier wavelength, the channel response vectors $\boldsymbol{h}_{\rm r}(\theta_{i,p})$ and $\boldsymbol{h}_{\rm t}(\varphi_{i,p})$ for the $p$-th sub-path with the angle-of-arrival (AoA) $\theta_{i,p}$ at the user and the angle-of-departure (AoD) $\varphi_{i,p}$ at the BS can be written as

$$\boldsymbol{h}_{\rm r}(\theta_{i,p}) = \left[1\ e^{-{\rm j}\pi\cos\theta_{i,p}}\cdots e^{-{\rm j}\pi(M_{\rm r}-1)\cos\theta_{i,p}}\right]^{\rm T}, \quad (3)$$

$$\boldsymbol{h}_{\rm t}(\varphi_{i,p}) = \left[1\ e^{-{\rm j}\pi\cos\varphi_{i,p}}\cdots e^{-{\rm j}\pi(M_{\rm t}-1)\cos\varphi_{i,p}}\right]^{\rm T}, \quad (4)$$

In typical mmWave scenario, LoS channel is dominant with fewer number of NLoS sub-paths $P$ [23]. Meanwhile, due to the relatively larger path-loss of NLoS sub-paths, $|\alpha_0|$ is 5dB to 10dB stronger than $|\alpha_p|, 1 \leq p \leq P$ [23].

### B. Problem Formulation

Here, denoting $\boldsymbol{h}_i = \boldsymbol{h}_{\rm t}(\varphi_{i,0})$ and adopting the conjugate beamforming/combining, we have $\boldsymbol{f}_i = \frac{1}{\sqrt{M_{\rm t}}}\boldsymbol{h}_i^*$ and $\boldsymbol{w}_i = \frac{1}{\sqrt{M_{\rm r}}}\boldsymbol{h}_r^*(\theta_i)$, where $(\cdot)^*$ denotes the conjugate operator. Considering the symmetry of the two users, the achievable average downlink SE $C_2$ is formulated as

$$C_2 = \log_2\left(1 + \frac{M_{\rm t}M_{\rm r}}{M_{\rm r}|\boldsymbol{h}_1^{\rm T}\boldsymbol{f}_2|^2 + \sigma_n^2}\right). \quad (5)$$

Note that the asymptotic orthogonality of conventional massive MIMO is invalid here because of the high correlation between the LoS channels $\boldsymbol{h}_1$ and $\boldsymbol{h}_2$, which produces severe IUI, reducing the downlink SE considerably. Furthermore, the following fact stated in Lemma 1 does not seem to be widely recognized.

*Lemma 1:* For strong LoS channels, employing as many as possible transmit antennas is generally a bad choice.

By denoting $\varepsilon = |\cos\varphi_1 - \cos\varphi_2|$, the magnitude of the IUI $|\boldsymbol{h}_1^{\rm T}\boldsymbol{f}_2|$ is given as

$$\begin{aligned}|\boldsymbol{h}_1^{\rm T}\boldsymbol{f}_2| &= \frac{1}{\sqrt{M_{\rm t}}}\left|\sum_{m=0}^{M_{\rm t}} e^{{\rm j}\pi m\varepsilon}\right| = \frac{1}{\sqrt{M_{\rm t}}}\left|\frac{1-e^{{\rm j}\pi M_{\rm t}\varepsilon}}{1-e^{{\rm j}\pi\varepsilon}}\right| \\ &= \frac{1}{\sqrt{M_{\rm t}}}\left|\frac{\sin\frac{\pi M_{\rm t}\varepsilon}{2}}{\sin\frac{\pi\varepsilon}{2}}\right| \triangleq \frac{1}{\sqrt{M_{\rm t}}}A(M_{\rm t},\varepsilon) \\ &= \frac{\sqrt{M_{\rm t}}}{\left|{\rm sinc}\frac{\pi\varepsilon}{2}\right|}\left|{\rm sinc}\frac{\pi M_{\rm t}\varepsilon}{2}\right| \to \sqrt{M_{\rm t}},\ \varepsilon \to 0. \end{aligned} \quad (6)$$

This article has been accepted for publication in a future issue of this journal, but has not been fully edited. Content may change prior to final publication. Citation information: DOI 10.1109/ACCESS.2018.2872953, IEEE Access



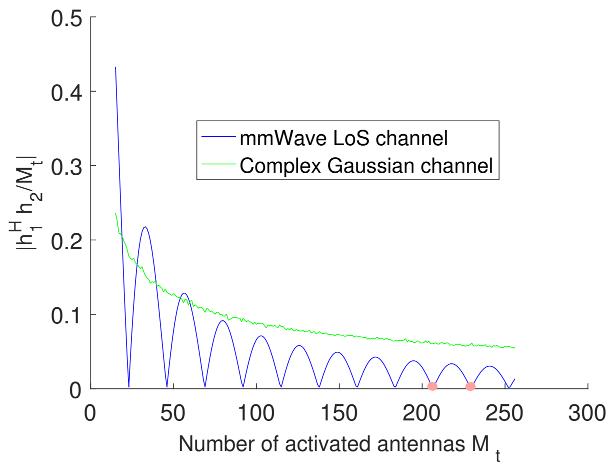


Fig. 1. Comparison of the correlations for the mmWave LoS and complex Gaussian NLoS channels.

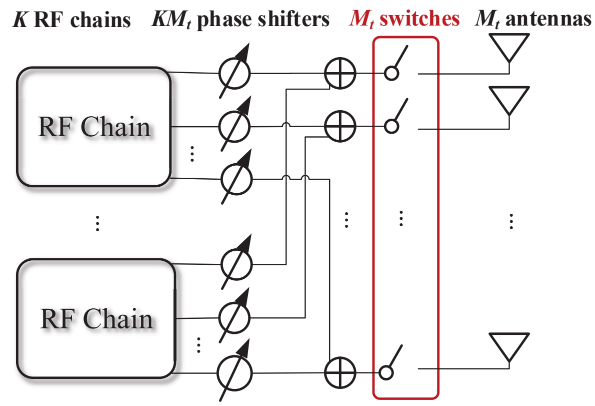


Fig. 2. Analogue beamforming structure: for conventional CB, all the $M_{\rm t}$ switches are closed, while for PACB, only the first $N$ switches are closed.

Thus, employing more transmit antennas may lead to higher interference, particularly when the two users are adjacent.

The correlations of the two users' channel vectors, $\boldsymbol{h}_1$ and $\boldsymbol{h}_2$, as the function of $M_{\rm t}$ under the LoS and NLoS conditions, respectively, are compared in Fig. 1, where the two users' AoDs are $\varphi_1 = 90^\circ$ and $\varphi_2 = 85^\circ$, respectively. In the NLoS MIMO with complex Gaussian channel, the correlation between two channel vectors is reduced monotonously with the increase of $M_{\rm t}$, and the asymptotic orthogonality is only achieved as $M_{\rm t} \to \infty$. Furthermore, the achievable performance of employing $N = 206$ transmit antennas is worst than that achieved by employing all the $M_{\rm t} = 256$ antennas. By contrast, in the LoS channel condition, the correlation exhibits oscillating and damping as $M_{\rm t}$ increases, and it also becomes zero with specific final $M_{\rm t}$ values, e.g., red points. Consequently, employing $N = 206$ transmit antennas outperforms the case of employing all the $M_{\rm t} = 256$ antennas.

*Remark 1*: The actual amount of IUI does not depend on the number of transmit antennas $M_{\rm t}$ alone. Rather, it is determined by the product of $M_{\rm t}$ and $\varepsilon$, the latter specifying the spatial structure of LoS channels. The sinc function is quasi-periodic with many zero cross points. It can readily be seen that if $\frac{\pi M_{\rm t}\varepsilon}{2}$ happens to be such a zero cross point, the IUI vanishes. This motivates our PACB. Specifically, rather than activating all the $M_{\rm t}$ transmit antennas as in the conventional CB, we only activate a fraction of the antennas, say $N$ antennas, where obviously $2 \le N \le M_{\rm t}$. By choosing an appropriate $N$, we can let $\frac{\pi N\varepsilon}{2}$ to be at or near a zero cross point of the sinc function, and this will dramatically reduce the IUI.

## III. Proposed Scheme

### A. *Partially-Activated Conjugate Beamforming*

The transmitter structures of the conventional CB and the proposed PACB are both depicted in Fig. 2. Assuming $K$ RF chains, $KM_{\rm t}$ phase shifters are utilized to perform the analogue beamforming based on the full-connection structure [9]. For the conventional CB, all the $M_{\rm t}$ transmit antennas are activated, corresponding to close all the $M_{\rm t}$ switches in Fig. 2. By contrast, the PACB only activates the first $N$ antennas, which corresponds to close the first $N$ switches in Fig. 2. Hence, the PACB vector $\boldsymbol{f}_i$ is expressed as

$$\boldsymbol{f}_i = \frac{1}{\sqrt{N}}\left[1 \; e^{\mathrm{j}\pi\cos\varphi_i} \cdots e^{\mathrm{j}\pi(N-1)\cos\varphi_i} \; \mathbf{0}_{(M_{\rm t}-N)\times 1}^{\rm T}\right]^{\rm T}, \quad (7)$$

where the $(M_{\rm t}-N)\times 1$ zero vector $\mathbf{0}_{(M_{\rm t}-N)\times 1}$ indicates that the corresponding antenna elements $N \le m \le M_{\rm t}-1$ are turned off. We first assume the two-user case. Substituting $\boldsymbol{f}_i$ of (7) for $i = 1, 2$ into (5) yields

$$C_2(N) = \log_2\left(1 + \frac{1}{\frac{1}{N^2}A(N,\varepsilon)^2 + \frac{1}{NM_{\rm r}}\sigma_n^2}\right). \quad (8)$$

The optimal number of activated antennas, $N_{\rm o}$, which maximizes the capacity $C_2(N)$ of (8), is obtained as follows

$$N_{\rm o} = \arg\max_{2\le N\le M_{\rm t}} C_2(N). \quad (9)$$

The exhaustive search with the complexity on the order of $\mathsf{O}(M_{\rm t})$ can be employed to calculate $N_{\rm o}$.

*Remark 2*: Unlike the average SE of the NLoS massive MIMO, which is monotonously increasing with $M_{\rm t}$, the average SE of the LoS massive MIMO exhibits the oscillating and increasing characteristics as $M_{\rm t}$ increases, owing to its IUI characteristics shown in Fig. 1. Fig. 3 compares the average downlink SEs of the mmWave LoS and complex Gaussian NLoS channels, where the two users' AoDs are $\varphi_1 = 90^\circ$ and $\varphi_2 = 85^\circ$, respectively, while the AWGN power is $\sigma_n^2 = 1$. Observe that $N_{\rm o} = 252$, which is smaller than $M_{\rm t} = 256$. In fact, even by only activating first $N = 22$ antennas, we have $C_2(22) > C_2(256)$, which is remarkable.

It is highly desired to derive an even lower complexity search algorithm, particularly, if the solution found by such a low-complexity algorithm is at least a near optimal solution. Let us consider the two special cases of (9).

1) In extremely high noisy scenarios, where the noise is dominant and the interference is small by comparison, the SINR can be approximated by the SNR of $\frac{NM_{\rm r}}{\sigma_n^2}$, which indicates

This article has been accepted for publication in a future issue of this journal, but has not been fully edited. Content may change prior to final publication. Citation information: DOI 10.1109/ACCESS.2018.2872953, IEEE Access



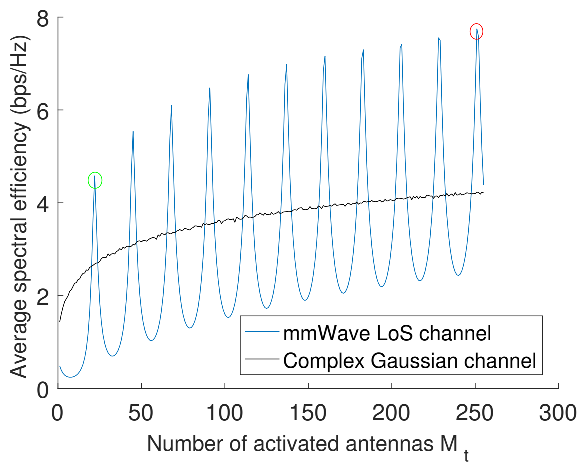


Fig. 3. Comparison of the average downlink capacities for the mmWave LoS and complex Gaussian NLoS channels.

that the optimal solution to the optimization problem (9) is approximately $N_{\rm o} = M_{\rm t}$, the fully activated beamforming.

2) In massive MIMO, the IUI is generally dominant and the effect of the noise is negligible by comparison. Hence, the SINR can be approximated by the SIR. This indicates that a suboptimal solution $N_{\rm s}$ to the optimization problem (9) can be obtained as the solution of the following optimization

$$N_{\rm s} = \arg \max_{2 \le N \le M_{\rm t}} \frac{N}{A(N,\varepsilon)} = \arg \max_{2 \le N \le M_{\rm t}} \left| \frac{N \sin \frac{\pi\varepsilon}{2}}{\sin \frac{\pi N \varepsilon}{2}} \right|. \quad (10)$$

The optimization (10) is equivalent to the optimization (9) by neglecting the noise power in the capacity formula (8).

### B. Low-Complexity Searching Algorithm

Since the denominator $\sin \frac{\pi N \varepsilon}{2}$ in the optimization (10) is quasi-periodic, we can select the value of $N_{\rm s}$ to let $\sin \frac{\pi N_{\rm s} \varepsilon}{2} \to 0$ in order to reduce the IUI dramatically. Ignoring the effect of the linear factor $N$, (10) can be further expressed as

$$N_{\rm s} = \arg \min_{2 \le N \le M_{\rm t}} \left| \sin \frac{\pi N \varepsilon}{2} \right|. \quad (11)$$

The solution to the optimization (11) is to let $\frac{N\varepsilon}{2}$ be the closest to an integer, specifically,

$$N_{\rm s} = \arg \min_{2 \le N \le M_{\rm t}} \left| \frac{N\varepsilon}{2} - \left\lfloor \frac{N\varepsilon}{2} \right\rceil \right|, \quad (12)$$

where the operator $\lfloor \cdot \rceil$ denotes the proximal integer. Since $\varepsilon$ is small and in the limit case $\varepsilon \to 0$, we can express $\frac{2}{\varepsilon} = T + t$, in which $t$ denotes the fractional part and

$$T = \left\lfloor \frac{2}{\varepsilon} \right\rfloor \ge 1 \quad (13)$$

is the integer part, where $\lfloor \cdot \rfloor$ stands for the integer floor operator. Further denote the residual function

$$q(N) = \left| \frac{N\varepsilon}{2} - \left\lfloor \frac{N\varepsilon}{2} \right\rceil \right|. \quad (14)$$

Clearly, we can decompose $N$ into

$$N = nT + l, \quad (15)$$

where $n$ is the index of the periodicity with period $T$ and $0 \le l \le T-1$ is the remainder. Then $q(N)$ can be simplified as

$$\begin{aligned} q(N) =& q(nT+l) = \left| \frac{nT\varepsilon}{2} + \frac{l\varepsilon}{2} - \left\lfloor \frac{nT\varepsilon}{2} + \frac{l\varepsilon}{2} \right\rceil \right| \\ =& \left| n\left(\frac{2}{\varepsilon} - t\right)\frac{\varepsilon}{2} + \frac{l\varepsilon}{2} - \left\lfloor n\left(\frac{2}{\varepsilon} - t\right)\frac{\varepsilon}{2} + \frac{l\varepsilon}{2} \right\rceil \right| \\ =& \left| (l-nt)\frac{\varepsilon}{2} - \left\lfloor (l-nt)\frac{\varepsilon}{2} \right\rceil \right| = \left| \frac{l-nt}{T+t} - \left\lfloor \frac{l-nt}{T+t} \right\rceil \right|. \end{aligned} \quad (16)$$

Similarly, we can decompose $\frac{nt}{T+t}$ into the two parts as

$$\begin{aligned} \frac{nt}{T+t} =& \left\lfloor \frac{nt}{T+t} \right\rceil + \left( \frac{nt}{T+t} - \left\lfloor \frac{nt}{T+t} \right\rceil \right) \\ \triangleq & G(n) + g(n), \end{aligned} \quad (17)$$

with $G(n)$ and $g(n)$ denoting the integer part and fractional part, respectively. Substituting (17) to (16) yields

$$q(N) = \left| \frac{l}{T+t} - g(n) - \left\lfloor \frac{l}{T+t} - g(n) \right\rceil \right|. \quad (18)$$

Considering $0 \le \frac{l}{T+t} < 1$ and $0 \le g(n) < 1$, we have

$$b(l,n) = \frac{l}{T+t} - g(n) \in (-1,\ 1). \quad (19)$$

Therefore, (18) can be rewritten as

$$q(N) = \begin{cases} 1 + b(l,n), & b(l,n) \in \big(-1,\ -\frac{1}{2}\big), \\ -b(l,n), & b(l,n) \in \big[-\frac{1}{2},\ 0\big), \\ b(l,n), & b(l,n) \in \big[0,\ \frac{1}{2}\big), \\ 1 - b(l,n), & b(l,n) \in \big[\frac{1}{2},\ 1\big). \end{cases} \quad (20)$$

Given the index of periodicity $n$, we have $0 \le l \le T-1$, and $b(l,n)$ takes the value from the finite set of $T$ values, namely,

$$b(l,n) \in \left\{ -g(n), \frac{1}{T+t} - g(n), \cdots, \frac{T-1}{T+t} - g(n) \right\}, \quad (21)$$

where $-g(n) \le 0$ and $\frac{T-1}{T+t} - g(n) < 1$. Further observe from (20) that $q(N)$ attains its local-minimum when $b(l,n) \to -1$, 0 or 1. Therefore, the possible candidates of $l$ to achieve the minimum of $q(N)$ can be obtained only on the boundaries with $l = 0,\ T-1,\ l_n^-$ or $l_n^+$, where $l_n^+ = l_n^- + 1$, satisfying

$$\frac{l_n^-}{T+t} - g(n) < 0 < \frac{l_n^+}{T+t} - g(n). \quad (22)$$

First, consider the potential candidates $l_n^-$ and $l_n^+$ by defining

$$q(N_n) = \min\left\{ q(nT + l_n^-), q(nT + l_n^+) \right\}. \quad (23)$$

Since the length of the interval $\left[ \frac{l_n^-}{T+t} - g(n),\ \frac{l_n^+}{T+t} - g(n) \right]$ is $\frac{1}{T+t}$, $q(N_n)$ is upper bounded by $\frac{1}{2(T+t)}$, that is,

$$q(N_n) \le \frac{1}{2(T+t)} = \frac{\varepsilon}{4}. \quad (24)$$

Next, consider the other two potential candidates $l = 0$ and $T$. At $l = 0$ or $T$, $q(N)$ depends on the fractional part $g(n)$, which follows the uniform distribution in $[0,\ 1)$ and, therefore,

This article has been accepted for publication in a future issue of this journal, but has not been fully edited. Content may change prior to final publication. Citation information: DOI 10.1109/ACCESS.2018.2872953, IEEE Access



has the average value of 0.5. Thus, at $l = 0$ or $T$ the value of $q(N)$ is typically much larger than $\frac{\varepsilon}{4}$. Consequently, we can rule out $l = 0$ and $T$. Hence, given $n$, the single local-minimum solution is at $l = l_n^-$ or $l_n^+$, specified by (23).

Once we have $l_n^-$ and $l_n^+$, the next pair of indexes $l_{n+1}^-$ and $l_{n+1}^+$ can be obtained by the forward recursion. Specifically, based on (17), $g(n+1)$ is calculated by

$$\begin{aligned} g(n+1) &= g(n) + \frac{t}{T+t} - \left\lfloor g(n) + \frac{t}{T+t} \right\rfloor \\ &= \begin{cases} g(n) + \frac{t}{T+t}, & G(n+1) = G(n), \\ g(n) + \frac{t}{T+t} - 1, & G(n+1) = G(n) + 1. \end{cases} \end{aligned} \tag{25}$$

As for the first condition with $G(n+1) = G(n)$, we have

$$\begin{aligned} &\frac{l_{n+1}^-}{T+t} - g(n+1) < 0 < \frac{l_{n+1}^+}{T+t} - g(n+1) \\ \Leftrightarrow &\frac{l_{n+1}^- - 1}{T+t} - g(n) < 0 < \frac{l_{n+1}^+ - 1}{T+t} - g(n) \\ \Leftrightarrow &\, l_{n+1}^- - 1 \le l_n^- \text{ and } l_{n+1}^+ - 1 \ge l_n^+. \end{aligned} \tag{26}$$

Considering $l_n^+ = l_n^- + 1$, we obtain

$$l_{n+1}^- = l_n^+ \text{ and } l_{n+1}^+ = l_n^+ + 1. \tag{27}$$

Under the second condition with $G(n+1) = G(n)+1$, similar to (26), $l_{n+1}^-$ satisfies

$$l_n^+ + (T+t) \le l_{n+1}^- \le l_n^- + (T+t) + 1. \tag{28}$$

Restricting $0 \le l \le T-1$, the forward recursions in (27) and (28) can be collectively formulated as

$$l_{n+1}^- = l_n^+ \text{ and } l_{n+1}^+ = \left(l_n^+ + 1\right) \mod T, \tag{29}$$

where $\mod$ stands for the modulo operator.

Starting from the initial index $n = 1$ with $l_1^- = 0$, therefore, we can obtain all the candidate indexes by the forward recursion (29) and consequently derive the candidate set

$$\mathbb{S} = \left\{N_n | N_n \text{ given by } (23)\right\}. \tag{30}$$

It is obvious from the above derivation that the optimization (10) is identical to the following optimization

$$N_\mathrm{s} = \arg\max_{N \in \mathbb{S}} \frac{N}{A(N, \varepsilon)}. \tag{31}$$

The complexity of solving the optimization (31) is on the order of $\mathsf{O}(|\mathbb{S}|)$, where $|\mathbb{S}|$ is the cardinal of $\mathbb{S}$. For small $\varepsilon$, $T$ is large and we have $|\mathbb{S}| \approx \frac{M_\mathrm{t}}{T} \ll M_\mathrm{t}$. Therefore, our low-complexity search imposes much lower complexity than the exhaustive search to find a near optimal solution $N_\mathrm{s}$. For example, when $\varphi_1 = 90°$ and $\varphi_2 = 85°$, we have $\varepsilon = 0.0872$ and $T = 22$, which means that the complexity is at least one order of magnitude lower than the exhaustive search.

## C. Performance Analysis

As pointed out previously, with all the $M_\mathrm{t}$ transmit antennas activated, the magnitude of the IUI $\frac{1}{\sqrt{M_\mathrm{t}}} A(M_\mathrm{t}, \varepsilon)$ is typically large, especially when $\varepsilon$ is small, i.e., the two users are close. The PACB, by activating only the $N_\mathrm{s}$ transmit antennas, reduces the IUI $\frac{1}{\sqrt{N_\mathrm{s}}} A(N_\mathrm{s}, \varepsilon)$ dramatically. An upper-bound of $\frac{1}{\sqrt{N_\mathrm{s}}} A(N_\mathrm{s}, \varepsilon)$ is derived as follows. Noting (24), we have

$$\begin{aligned} \left|\sin \frac{\pi N_\mathrm{s} \varepsilon}{2}\right| &= \left|\sin \pi \left(\left\lfloor \frac{N_\mathrm{s} \varepsilon}{2} \right\rceil \pm q(N_\mathrm{s})\right)\right| \\ &= \sin \pi q(N_\mathrm{s}) \le \sin \frac{\pi \varepsilon}{4}. \end{aligned} \tag{32}$$

Therefore, we have

$$\begin{aligned} \frac{1}{\sqrt{N_\mathrm{s}}} A(N_\mathrm{s}, \varepsilon) =& \frac{1}{\sqrt{N_\mathrm{s}}} \left| \frac{\sin \frac{\pi N_\mathrm{s} \varepsilon}{2}}{\sin \frac{\pi \varepsilon}{2}} \right| \le \frac{1}{\sqrt{N_\mathrm{s}}} \left| \frac{\sin \frac{\pi \varepsilon}{4}}{\sin \frac{\pi \varepsilon}{2}} \right| \\ \approx& \frac{1}{2\sqrt{N_\mathrm{s}}}, \end{aligned} \tag{33}$$

where the approximation is due to $\sin \varepsilon \to \varepsilon$ with $\varepsilon \to 0$. It can readily be seen that typically

$$\frac{1}{\sqrt{N_\mathrm{s}}} A(N_\mathrm{s}, \varepsilon) \ll \frac{1}{\sqrt{M_\mathrm{t}}} A(M_\mathrm{t}, \varepsilon). \tag{34}$$

Denote the downlink SEs achieved by $M_\mathrm{t}$, $N_\mathrm{s}$ and $N_\mathrm{o}$ as $C_\mathrm{f} = C_2(M_\mathrm{t})$, $C_\mathrm{s} = C_2(N_\mathrm{s})$ and $C_\mathrm{o} = C_2(N_\mathrm{o})$, respectively. Although the noise power $\frac{1}{N_\mathrm{s} M_\mathrm{r}} \sigma_n^2$ in the PACB is slightly larger than the noise power $\frac{1}{M_\mathrm{t} M_\mathrm{r}} \sigma_n^2$ in the fully activated case, its IUI power $\frac{1}{N_\mathrm{s}^2} A^2(N_\mathrm{s}, \varepsilon)$ is significantly lower than $\frac{1}{M_\mathrm{t}^2} A^2(M_\mathrm{t}, \varepsilon)$. Since the interference power is much larger than the noise power, we can conclude that $C_\mathrm{s} \gg C_\mathrm{f}$, except in the high noise case. It can also easily be seen that $C_\mathrm{s} \le C_\mathrm{o}$, and the equality holds when $\sigma_n^2 \to 0$. Since the system is interference limited, $C_\mathrm{s}$ is very close to $C_\mathrm{o}$, that is, $C_\mathrm{s} \approx C_\mathrm{o}$.

Furthermore, some insights about the effect of $\varepsilon$ on $N_\mathrm{s}$ are provided. Based on the forward recursion in (29), the candidate $N_\mathrm{s}$ occurs quasi-periodically with period $T$. Moreover, to guarantee sufficient power of received signal, the largest $N_\mathrm{s}$ candidate in $\mathbb{S}$ is preferred. Therefore, although we cannot obtain the exact value of $N_\mathrm{s}$ explicitly, we have the following constrain on $N_\mathrm{s}$,

$$N_\mathrm{s} \ge M_\mathrm{t} - T = M_\mathrm{t} - \left\lfloor \frac{2}{\varepsilon} \right\rceil, \tag{35}$$

which indicates that $N_\mathrm{s}$ is closer to $M_\mathrm{t}$ with relatively larger $\varepsilon$. For example, equipping $M_\mathrm{t} = 256$ antennas at the BS and assuming $\varphi_1 = 90°$, $\varphi_2 = 85°$, we have $T = 22$ and $N_\mathrm{s} = 252$. As comparison, if $\varphi_1 = 90°$, $\varphi_2 = 88°$, we obtain $T = 57$ and $N_\mathrm{s} = 228$.

Next, the SE averaged over the distribution of AoDs is presented. Combining (8) with (33) and ignoring the effect of noise, we have the lower-bound as

$$C_2(N_\mathrm{s}) \ge \log_2 \left(1 + 4N_\mathrm{s}^2 \cos^2 \frac{\pi \varepsilon}{4}\right), \tag{36}$$

Due to the analytical difficulty of directly calculating the expectation of $C_2(N_\mathrm{s})$ over different $\varphi_1, \varphi_2$, we turn to focus on the average SE over various $\varepsilon$ to address this point. Specifically, $\varepsilon$ is assumed uniformly distributed in $(\varepsilon_{\min}, \varepsilon_{\max})$. Hence,

$E\{C_2(N_{\mathrm{s}})\}$ can be expressed as

$$\begin{aligned}E\{C_2(N_{\mathrm{s}})\} &= \frac{1}{\varepsilon_{\max}-\varepsilon_{\min}}\int_{\varepsilon_{\min}}^{\varepsilon_{\max}}\log_2\Big(1+4N_{\mathrm{s}}^2\cos^2\frac{\pi\varepsilon}{4}\Big)d\varepsilon \\ &\geq \frac{2}{\varepsilon_{\max}-\varepsilon_{\min}}\int_{\varepsilon_{\min}}^{\varepsilon_{\max}}\Big(\log_2 2N_{\mathrm{s}}+\log_2\cos\frac{\pi\varepsilon}{4}\Big)d\varepsilon \\ &\overset{(a)}{\geq} 2\log_2 2(M_{\mathrm{t}}-T_{\min}) \\ &\quad+\frac{2}{\varepsilon_{\max}-\varepsilon_{\min}}\int_{\varepsilon_{\min}}^{\varepsilon_{\max}}\log_2\cos\frac{\pi\varepsilon}{4}d\varepsilon \\ &\overset{(b)}{\geq} 2\log_2 2(M_{\mathrm{t}}-T_{\min})-\frac{4}{\varepsilon_{\max}-\varepsilon_{\min}}\end{aligned} \tag{37}$$

wherein (a) is given from (35) by denoting $T_{\min}=\lfloor\frac{2}{\varepsilon_{\min}}\rfloor$ as the periodic of $N_{\mathrm{s}}$ with $\varepsilon_{\min}$. (b) is valid because of $\varepsilon\in(\varepsilon_{\min},\varepsilon_{\max})\subset(0,2)$ and the definite integral $\int_0^{\pi/2}\ln\cos x dx=-\frac{\pi}{2}\ln 2$. Observed from (37), we find that the proposed PACB is capable of providing sufficient spatial multiplexing gain offered by large-scale antenna array at the BS. This result proves that PACB is still adequately valid when considering the effect of AoD distribution, not just for the case of adjacent users discussed above.

### D. Analyses for AoD estimation error

Denoting $\varepsilon'=\varepsilon+\Delta\varepsilon$, wherein $\Delta\varepsilon$ represents the AoD gap error caused by AoD estimation error, BS calculates the corresponding number of activated antennas $N_{\mathrm{s}}'$ and average SE $C_2(N_{\mathrm{s}}')$. Generally, $\Delta\varepsilon/\varepsilon\ll 1$ is assumed, which is reasonable by adopting large-scale antenna array at the BS along with advanced AoD estimation methodologies [24]. Similar to (32), we have

$$\begin{aligned}\Big|\sin\frac{\pi N_{\mathrm{s}}'\varepsilon}{2}\Big| &= \Big|\sin\pi\Big(q(N_{\mathrm{s}}')\pm\Big\lfloor\frac{N_{\mathrm{s}}'\varepsilon'}{2}\Big\rceil-\frac{N_{\mathrm{s}}'\Delta\varepsilon}{2}\Big)\Big| \\ &= \Big|\sin\pi\Big(q(N_{\mathrm{s}}')-\frac{N_{\mathrm{s}}'\Delta\varepsilon}{2}\Big)\Big| \\ &\leq \Big|\sin\pi q(N_{\mathrm{s}}')\Big|\Big|\cos\frac{\pi N_{\mathrm{s}}'\Delta\varepsilon}{2}\Big| \\ &\quad+\Big|\cos\pi q(N_{\mathrm{s}}')\Big|\Big|\sin\frac{\pi N_{\mathrm{s}}'\Delta\varepsilon}{2}\Big| \\ &\leq \frac{\pi\varepsilon'}{4}+\Big|\frac{\pi N_{\mathrm{s}}'\Delta\varepsilon}{2}\Big|.\end{aligned} \tag{38}$$

Therefore, we have

$$\begin{aligned}\frac{1}{\sqrt{N_{\mathrm{s}}'}}A(N_{\mathrm{s}}',\varepsilon) &\leq \frac{1}{\sqrt{N_{\mathrm{s}}'}}\left|\frac{\frac{\pi\varepsilon'}{4}+\Big|\frac{\pi N_{\mathrm{s}}'\Delta\varepsilon}{2}\Big|}{\sin\frac{\pi\varepsilon}{2}}\right| \\ &\approx \frac{1}{\sqrt{N_{\mathrm{s}}'}}\big(0.5+(0.5+N_{\mathrm{s}}')\frac{\Delta\varepsilon}{\varepsilon}\big),\end{aligned} \tag{39}$$

which is readily smaller than $\frac{1}{\sqrt{M_{\mathrm{t}}}}A(M_{\mathrm{t}},\varepsilon)$ with conventional CB and indicates lower IUI between two users.

*Remark 3*: Readily, the proposed PACB still outperforms conventional CB with moderately small AoD estimation error in general cases. Moreover, a pre-detection can be added to avoid the performance degradation with large AoD estimation error and hence improves the robustness of the proposed PACB methodology. Specifically, if $C_2(N_{\mathrm{s}}')>C_{\mathrm{f}}$, BS activates $N_{\mathrm{s}}'$ antennas for beamforming, otherwise conventional CB is performed by activating all $M_{\mathrm{t}}$ antennas.

### E. PACB for $I>2$

The SINR of the $i$th user, where $1\leq i\leq I$, is

$$\mathrm{SINR}_i(N)=\frac{|\boldsymbol{h}_i^{\mathrm{T}}\boldsymbol{f}_i|^2}{\sum\limits_{l=1,l\neq i}^{I}|\boldsymbol{h}_i^{\mathrm{T}}\boldsymbol{f}_l|^2+\sigma_n^2}=\frac{N}{\sum\limits_{l=1,l\neq i}^{I}\frac{A(N,\varepsilon_{l,i})^2}{N}+\sigma_n^2}, \tag{40}$$

where $\varepsilon_{l,i}=|\cos\varphi_l-\cos\varphi_i|$. Thus the average downlink SE can be expressed as

$$C_I(N)=\frac{1}{I}\sum_{i=1}^{I}\log_2\big(1+\mathrm{SINR}_i(N)\big). \tag{41}$$

The optimal number of activated antennas, $N_{\mathrm{o}}$, is given by

$$N_{\mathrm{o}}=\arg\max_{2\leq N\leq M_{\mathrm{t}}}C_I(N). \tag{42}$$

The exhaustive search to find $N_{\mathrm{o}}$ has the complexity $\mathsf{O}(M_{\mathrm{t}})$.

Similar to (30), for each pair of users, we can derive the candidate set $\mathbb{S}_{i,l}=\{N_{i,l,n}\}$, where $1\leq i<l\leq I$. Then the intersection set of all the $\mathbb{S}_{i,l}$ is formed

$$\mathbb{S}=\bigcap_{1\leq i<l\leq I}\mathbb{S}_{i,l}. \tag{43}$$

To avoid $\mathbb{S}=\emptyset$, we perform a post-process on all the $\mathbb{S}_{i,l}$ as

$$\mathbb{S}_{i,l}=\big\{N\big||N-N_{i,l,n}|\leq\mu_{i,l}\big\}, \tag{44}$$

where $\mu_{i,l}$ is the offset for $\mathbb{S}_{i,l}$. By also including $N$ values that are close to $N_{i,l,n}$, the sets $\mathbb{S}_{i,l}$ are enlarged to ensure that $\mathbb{S}$ could not be an empty set. A near optimal solution to $N_{\mathrm{o}}$ can then be obtained by solving the optimization problem

$$N_{\mathrm{s}}=\arg\max_{N\in\mathbb{S}}\bar{C}_I(N), \tag{45}$$

where $\bar{C}_I(N)$ is the SE by ignoring the noise term in (40).

## IV. Simulation Results

We consider four two-user cases and one four-user case.

*A. Case One (two-user)*: The BS is equipped with $M_{\mathrm{t}}=128$ transmit antennas, while each of the two users employs $M_{\mathrm{r}}=16$ receive antennas. The system's normalized SNR is defined as $\mathrm{SNR}=1/\sigma_n^2$. The two AoDs $\varphi_1$ and $\varphi_2$ are generated to depict the scenario of two adjacent users. Specifically, $\varphi_2=\varphi_1+\delta$, where the difference in the AoDs $\delta$, representing the closeness of the two users, is uniformly distributed in $\big(0,\ 5^\circ\big)$.

Fig. 4 compares the downlink SEs achieved by the conventional CB and the PACB as the functions of SNR. Except for the extremely high noise situation, where the optimal solution is to activate all the antennas, i.e., $N_{\mathrm{o}}=M_{\mathrm{t}}$, we observe the significantly SE gain of the PACB over the conventional CB that activates all the $M_{\mathrm{t}}$ antennas. The higher the system's SNR is, the higher this gain becomes. With $\mathrm{SNR}=0\,\mathrm{dB}$, for example, $C_{\mathrm{s}}$ is 30% larger than $C_{\mathrm{f}}$. From Fig. 4, we also observe that except for the extremely high noise situation, $C_{\mathrm{s}}$ is indistinguishable from $C_{\mathrm{o}}$. This confirms the performance analysis presented in Section III-C, specifically, $C_{\mathrm{s}}\approx C_{\mathrm{o}}$.

*B. Case Two (two-user)*: In this case, we set $\mathrm{SNR}=0\,\mathrm{dB}$ and vary the number of transmit antennas $M_{\mathrm{t}}$. The rest of the system's parameters are as in *Case One*. Fig. 5 compares the

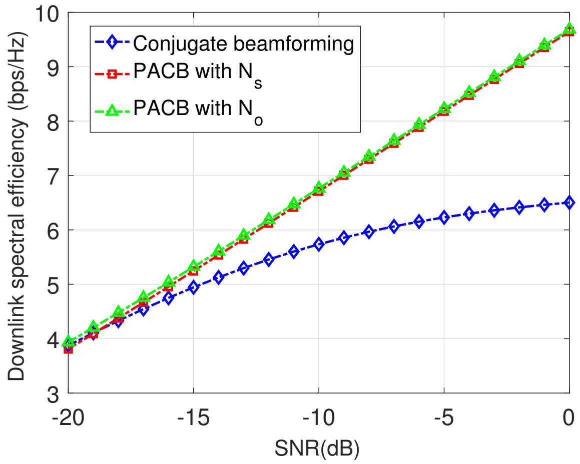


Fig. 4. Case one (two-user): comparison of average SE for different SNRs.

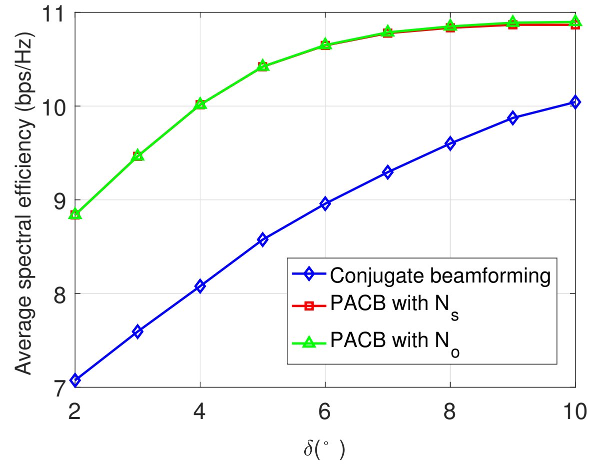


Fig. 6. Case three (two-user): comparison of average SE for various differences between the two AoDs.

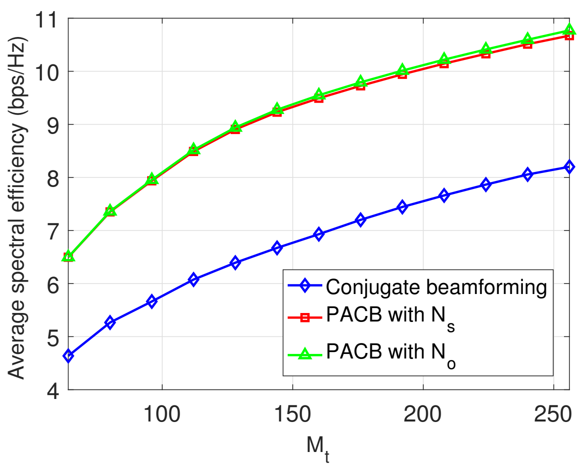


Fig. 5. Case two (two-user): comparison of average SE for different numbers of transmit antennas.

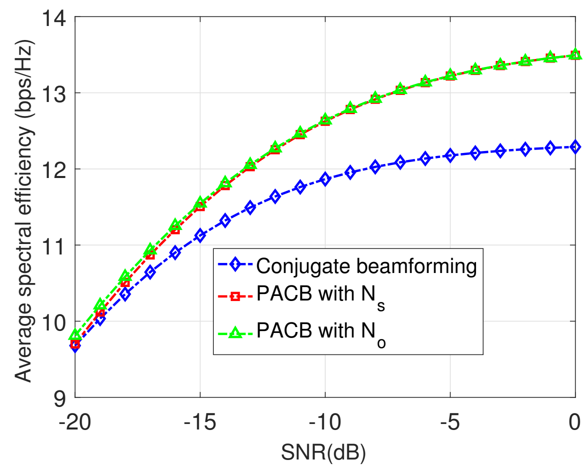


Fig. 7. Case four (four-user): comparison of average SE for different SNRs.

downlink SEs achieved by the conventional CB and the PACB as the functions of the number of transmit antennas. Observe that an average of 2 bps/Hz performance gain is attained by the PACB over the conventional CB. This further validates the theoretical analysis for $C_{\rm s} \gg C_{\rm f}$ presented in Section III-C. The results of Fig. 5 also confirm that $C_{\rm s} \approx C_{\rm o}$.

*C. Case Three (two-user)*: We then set SNR $= 0$ dB and vary $\delta$ from $2^\circ$ to $10^\circ$. The rest of the system's parameters are as in *Case One*. Observe from Fig. 6 that the performance of the conventional CB degrades quickly as $\delta$ decreases. This agrees with the analysis of Section II that the CB with all the $M_{\rm t}$ antennas activated is unable to handle the scenario of close users effectively. When $\delta$ decreases, $\varepsilon$ becomes smaller. As shown in Section II, as $\varepsilon \to 0$, the IUI suffered by the CB with all the $M_{\rm t}$ antennas activated approaches its maximum value. By contrast, observed from Fig. 6 that the performance gain of the proposed PACB scheme over the conventional CB increases as $\delta$ decreases. According to (24), the upper-bound of $q(N_{\rm s})$ approaches 0 as $\varepsilon \to 0$. Therefore, compared to the fixed residual $q(M_{\rm t})$, the IUI reduction capability of the PACB becomes more significant with smaller $\varepsilon$, which leads to larger performance gain over the conventional CB.

*D. Case Four (four-user)*: Again the BS is equipped with $M_{\rm t} = 128$ transmit antennas, while each of the four users employs $M_{\rm r} = 16$ receive antennas. The four users' AoDs, $\varphi_i$ for $1 \le i \le 4$, are related by $\varphi_i = \varphi_1 + \delta_i$, $i = 2, 3, 4$, where all the three $\delta_i$ are uniformly distributed in $\left(0,\ 5^\circ\right)$. Fig. 7 compares the downlink SEs achieved by the conventional CB and the PACB as the functions of SNR. As in *Case One* with two users, it can be seen that the PACB significantly outperforms the conventional CB.

*E. Case Five (two-user)*: Besides the above results obtained under pure LoS channels, additional comparisons of average spectral efficiency assuming different numbers of NLoS sub-paths are presented in Fig. 8, in which $P = 3, 6$ and $E\{|\alpha_0|\}/E\{|\alpha_p|\} = 10$dB are adopted. Obviously, the average spectral efficiency degenerates with more numbers of NLoS sub-paths. However, the PACB still outperforms the conven-

This article has been accepted for publication in a future issue of this journal, but has not been fully edited. Content may change prior to final publication. Citation information: DOI 10.1109/ACCESS.2018.2872953, IEEE Access



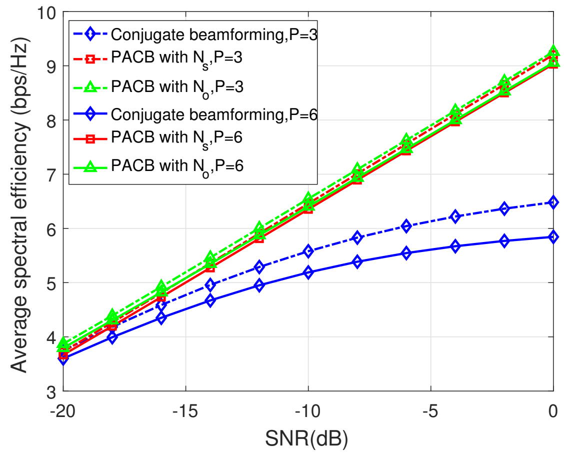


Fig. 8. Case five (two-user): comparison of average SE for different numbers of NLoS sub-paths.

tional CB considerably with different numbers of NLoS sub-paths.

## V. Conclusions

The PACB scheme has been proposed for LoS-dominant massive communication systems, especially with adjacent users. By exploiting the structure of LoS channel, the proposed PACB activates only a fraction of the transmit antennas for beamforming, and the optimal number of activated antennas can be determined by maximizing the system's downlink capacity using an exhaustive search, which has the complexity that is linear to the number of total available antennas. Alternatively, we have derived an even lower complexity searching algorithm to determine the number of activated antennas by maximizing the system's SIR only. Both theoretical analysis and simulation investigation have shown that the performance achieved by the PACB with this low-complexity search algorithm is indistinguishable from that achieved by the optimal PACB solution. More importantly, both theoretical analysis and simulation results have demonstrated that the PACB scheme offers significantly higher downlink spectral efficiency compared to the conventional conjugate beamforming counterpart.

## References

[1] F. Rusek, *et al.*, "Scaling up MIMO: opportunities and challenges with very large arrays," *IEEE Signal Process. Mag.*, vol. 30, no. 1, pp. 40–60, Jan. 2013.

[2] H. Q. Ngo, E. G. Larsson, and T. L. Marzetta, "Energy and spectral efficiency of very large multiuser MIMO systems," *IEEE Trans. Commun.*, vol. 61, no. 4, pp. 1436–1449, Apr. 2013.

[3] H. Yang, and T. L. Marzetta, "Performance of conjugate and zero-forcing beamforming in large-scale antenna systems," *IEEE J. Sel. Areas Commun.*, vol. 31, no. 2, pp. 172–179, Feb. 2013.

[4] E. Larsson, O. Edfors, F. Tufvesson, and T. Marzetta, "Massive MIMO for next generation wireless systems," *IEEE Commun. Mag.*, vol. 52, no. 2, pp. 186–195, Feb. 2014.

[5] O. N. Alrabadi, E. Tsakalaki, H. Huang, and G. F. Pedersen, "Beamforming via large and dense antenna arrays above a clutter," *IEEE J. Sel. Areas Commun.*, vol. 31, no. 2, pp. 314–325, Feb. 2013.

[6] J. Choi, "Multiuser precoding with limited cooperation for large-scale MIMO multicell downlink," *IEEE Trans. Wireless Commun.*, vol. 14, no. 3, pp. 1295–1308, 2015.

[7] S. K. Mohammed and E. G. Larsson, "Constant-envelope multi-user precoding for frequency-selective massive MIMO systems," *IEEE Commun. Letters*, vol. 2, no. 5, pp. 547–550, Oct. 2013.

[8] J. Zhang, S. Chen, R. G. Maunder, R. Zhang, and L. Hanzo, "Adaptive coding and modulation for large-scale antenna array based aeronautical communications in the presence of co-channel interference," *IEEE Trans. Wireless Commun.*, vol. 17, no. 2, pp. 1343–1357, Dec. 2017.

[9] Y. Zeng, R. Zhang, and T. J. Lim, "Wireless communications with unmanned aerial vehicles: opportunities and challenges," *IEEE Commun. Mag.*, vol. 54, no. 5, pp. 36–42, May 2016.

[10] T. J. Willink, C. C. Squires, G. W. K. Colman, and M. T. Muccio, "Measurement and characterization of low altitude air-to-ground MIMO channels," *IEEE Trans. Veh. Technol.*, vol. 65, no. 4, pp. 2637–2648, Apr. 2015.

[11] W. Roh. J.-Y. Seol, J. Park, B. Lee, J. Lee, Y. Kim, J. Cho, K. Cheun, and F. Aryanfar, "Millimeter-wave beamforming as an enabling technology for 5G cellular communications: theoretical feasibility and prototype results," *IEEE Commun. Mag.*, vol. 52, no. 3, pp. 106–113, Feb. 2014.

[12] A. L. Swindelhurst, E. Ayanoglu, P. Heydari, and F. Capolina, "Millimeter-wave massive MIMO: the next wireless revolution?" *IEEE Commun. Mag.*, vol. 52, no. 9, pp. 56–62, Sep. 2014.

[13] K. Guan, *et al.*, "On millimeter wave and THz mobile radio channel for smart rail mobility," *IEEE Trans. Veh. Technol.*, vol. 66, no. 7, pp. 5658–5674, Jul. 2017.

[14] O. El Ayach, S. Rajagopal, S. Abu-Surra, Z. Pi, and R. W. Heath, "Spatially sparse precoding in millimeter wave MIMO systems," *IEEE Trans. Wirel. Commun.*, vol. 13, no. 3, pp. 1499–1513, Mar. 2014.

[15] J.-C. Chen, "Efficient codebook-based beamforming algorithm for millimeter-wave massive MIMO systems," *IEEE Trans. Veh. Technol.*, vol. 66. no. 9, pp. 7809–7817, Sep. 2017.

[16] L. Liang, W. Xu, and X. Dong, "Low-complexity hybrid precoding in massive multiuser MIMO systems," *IEEE Wirel. Commun. Letters*, vol. 3, no. 6, pp. 653–656, Dec. 2014.

[17] R1-1609905, "MIMO transmission schemes for NR", InterDigital Communications, 3GPP TSG-RAN WG1 #86bis, Lisbon, Portugal, October 2016.

[18] M. Agiwal, A. Roy, and N. Saxena, "Next generation 5G wireless networks: a comprehensive survey", *IEEE Commun. Surveys Tuts*, vol. 18, no. 3, pp. 1617–1655, 3rd Quart., 2016

[19] R1-1701087, "On MU MIMO nonlinear precoding in NR", Nokia, Alcatel-Lucent Shanghai Bell, 3GPP TSG-RAN WG1 #Ad-Hoc, Spokane, USA, 16th-20th January 2017.

[20] P. Zhang, S. Chen, and L. Hanzo, "Two-tier channel estimation aided near-capcity MIMO transceivers relaying on norm-based joint transmit and receive antenna selection," *IEEE Trans. Wireless Commun.*, vol. 14, no. 1, pp. 122–137, Jan. 2015.

[21] N. N. Alotaibi and K. A. Hamdi, "Switched phased-array transmission architecture for secure millimeter-wave wireless communication," *IEEE Trans. Commun.*, vol. 64, no. 3, pp. 1303–1312, Mar. 2016.

[22] N. Valliappan, A. Lozano, and R. W. Heath, "Antenna subset modulation for secure millimeter-wave wireless communication," *IEEE Trans. Commun.*, vol. 61, no. 8, pp. 3231–3245, Aug. 2013.

[23] T. S. Rappaport, E. Ben-Dor, J. N. Murdock, and Y. Qiao, "38 GHz and 60 GHz angle-dependent propagation for cellular & peer-to-peer wireless communications," *in 2012 IEEE Int. Conf. on Communications (ICC)*, pp. 4568–4573, Jun. 2012.

[24] G. Zhu, K. Huang, V. K. N. Lau, B. Xia, X. Li, and S. Zhang, "Hybrid beamforming via the Kronecker decomposition for the millimeter-wave massive MIMO systems", *IEEE J. Sel. Areas Communi.*, vol. 35, no. 9, pp. 2097–2114, Sep. 2017.

**Wendong Liu** received the B.S. degree (Hons.) from Tsinghua University, Beijing, China, in 2015. He is currently pursuing the Ph.D. degree with the Department of Electronic Engineering, Tsinghua University. His research interests include massive MIMO, full-dimension MIMO and millimeter-wave communications.

This article has been accepted for publication in a future issue of this journal, but has not been fully edited. Content may change prior to final publication. Citation information: DOI 10.1109/ACCESS.2018.2872953, IEEE Access



**Zhaocheng Wang** (M'09-SM'11) received the B.S., M.S., and Ph.D. degrees from Tsinghua University, Beijing, China, in 1991, 1993, and 1996, respectively. From 1996 to 1997, he was a Postdoctoral Fellow with Nanyang Technological University, Singapore. From 1997 to 1999, he was with OKI Techno Centre (Singapore) Pte. Ltd., Singapore, where he was first a Research Engineer and later became a Senior Engineer. From 1999 to 2009, he was with Sony Deutschland GmbH, where he was first a Senior Engineer and later became a Principal Engineer. He is currently a Professor of Electronic Engineering with Tsinghua University and serves as the Director of Broadband Communication Key Laboratory, Tsinghua National Laboratory for Information Science and Technology (TNlist). He has authored or coauthored over 120 journal papers. He is the holder of 34 granted U.S./EU patents. He coauthored two books, one of which, Millimeter Wave Communication Systems, was selected by IEEE Series on Digital and Mobile Communication (Wiley-IEEE Press). His research interests include wireless communications, visible light communications, millimeterwave communications, and digital broadcasting. He is a Fellow of the Institution of Engineering and Technology. He served as the Associate Editor of IEEE Transactions on Wireless Communications (2011-2015) and the Associate Editor of IEEE Communications Letters (2013-2016), and has also served as Technical Program Committee Co-Chair of various international conferences.

**Jianfei Cao** received the B.S. degree from Hunan University, and the Ph.D. degree from Beijing Jiaotong University, China, in 2006 and 2012, respectively. From 2009 to 2010, he was a Visiting Ph.D. student with the University of Southampton, U.K. From 2012 to 2014, he was an Associated Researcher with NEC Laboratory, China. From 2014 to 2016, he was a Senior Engineer with Samsung Research Laboratory China. Since 2016, he has been a Vice-Manager with the SONY China Research Laboratory. His research interests include FD-MIMO in LTE and massive MIMO in 5G NR.

**Sheng Chen** (M'90-SM'97-F'08) received his BEng degree from the East China Petroleum Institute, Dongying, China, in 1982, and his PhD degree from the City University, London, in 1986, both in control engineering. In 2005, he was awarded the higher doctoral degree, Doctor of Sciences (DSc), from the University of Southampton, Southampton, UK.

From 1986 to 1999, He held research and academic appointments at the Universities of Sheffield, Edinburgh and Portsmouth, all in UK. Since 1999, he has been with School of Electronics and Computer Science, the University of Southampton, UK, where he currently holds the post of Professor in Intelligent Systems and Signal Processing. Dr Chen's research interests include adaptive signal processing, wireless communications, modelling and identification of nonlinear systems, neural network and machine learning, intelligent control system design, evolutionary computation methods and optimisation. He has published over 600 research papers. Dr. Chen is a Fellow of the United Kingdom Royal Academy of Engineering, a Fellow of IET, a Distinguished Adjunct Professor at King Abdulaziz University, Jeddah, Saudi Arabia, and an ISI highly cited researcher in engineering (March 2004). Professor Chen has 11,400 Web of Science citations and 24,000+ Google Scholar citations.

**Lajos Hanzo** FREng, FIEEE, FIET, Fellow of EURASIP, DSc received his degree in electronics in 1976 and his doctorate in 1983. In 2009 he was awarded an honorary doctorate by the Technical University of Budapest and in 2015 by the University of Edinburgh. In 2016 he was admitted to the Hungarian Academy of Science. During his 40-year career in telecommunications he has held various research and academic posts in Hungary, Germany and the UK. Since 1986 he has been with the School of Electronics and Computer Science, University of Southampton, UK, where he holds the chair in telecommunications. He has successfully supervised 111 PhD students, co-authored 18 John Wiley/IEEE Press books on mobile radio communications totalling in excess of 10 000 pages, published 1780 research contributions at IEEE Xplore, acted both as TPC and General Chair of IEEE conferences, presented keynote lectures and has been awarded a number of distinctions. Currently he is directing a 60-strong academic research team, working on a range of research projects in the field of wireless multimedia communications sponsored by industry, the Engineering and Physical Sciences Research Council (EPSRC) UK, the European Research Council's Advanced Fellow Grant and the Royal Society's Wolfson Research Merit Award. He is an enthusiastic supporter of industrial and academic liaison and he offers a range of industrial courses. He is also a Governor of the IEEE ComSoc and VTS. During 2008 - 2012 he was the Editor-in-Chief of the IEEE Press and a Chaired Professor also at Tsinghua University, Beijing.